RSC Advances

ROYAL SOCIETY OF CHEMISTRY

www.rsc.org/advances

High performance polydimethylsiloxane pervaporative membranes with hyperbranched polysiloxane as crosslinker for separation of *n*-butanol from water

Yunxiang Bai[1], Liangliang Dong[1], Jiaqiang Lin[1], Yuanhua Zhu[1], Chunfang Zhang[*1], Jin Gu[1], Yuping Sun[1], Youyi Xu[2]

[1]The Key Laboratory of Food Colloids and Biotechnology, Ministry of Education, School of Chemical and Material Engineering, Jiangnan University, Wuxi 214122, Jiangsu, China

[2]MOE Key Laboratory of Macromolecule Synthesis and Functionalization, Department of Polymer Science and Engineering, Zhejiang University, Hangzhou 310027, P. R. China

***Abstract*—**Hyperbranched polysiloxane (HPSiO) was successfully synthesized by a three-step process. The result of ^{29}Si Nuclear Magnetic Resonance (NMR) measurement indicates that the degree of branching (*DB*) of HPSiO is 0.73. Then, novel polysiloxane membranes, HPSiO-*c*-PDMS, were prepared by the cross-linking reaction between HPSiO and α,ω-dihydroxypolydimethylsiloxane (H-PDMS) with different molecular weights. HPSiO-*c*-PDMS membranes were firstly used as

* Corresponding author: E-mail address: zcf326@163.com., Tel: 86-510-85917090; Fax: 86-510-85917763.

membrane materials for recovering *n*-butanol from aqueous solution by pervaporation (PV). The HPSiO-*c*-PDMS membranes demonstrated high *n*-butanol/water selectivity as well as high permeability. As molecular weight of H-PDMS increased, the selectivity increased and *n*-butanol permeability of HPSiO-*c*-PDMS-2 (with moderate H-PDMS molecular weight) membrane showed the highest value. The effects of temperature and feed concentration on the PV performances were also investigated. The PV performance, *n*-butanol permeability and *n*-butanol/water selectivity of HPSiO-*c*-PDMS-2 membrane, reached 4.3×10^5 Barrer and 8.75, respectively, with a feed concentration of 1.0 wt% at 30 ^{o}C.

***Keywords*-**Hyperbranched polysiloxane; Pervaporation; *n*-Butanol; Membrane; Separation

1. Introduction

Increasing crude oil prices and extensive oil depletion over the past decades have stimulated both academic and industrial interests in producing biofuels (e.g. biobutanol and bioethanol) from renewable biomass by biotechnological processes [1,2]. Among alternative biofuels, biobutanol (*n*-butanol), having a higher fuel value, a lower volatility and a lower freezing point as compared with ethanol [3], is expected to play an important role in the next generation of biofuels. Biobutanol can be produced through conventional A-B-E (acetone-butanol-ethanol) fermentation using Clostridia bacteria (e.g. *Clostridium acetobutylicum or C. beijerinckii*) [4]. However, the low *n*-butanol tolerance of Clostridia bacteria leads to very dilute aqueous

solutions and thus high energy consumption during the product recovery, which makes the process economically uncompetitive with the petrochemical industry [5]. Therefore, the in-situ product removal with integrated separation processes has been proposed, including distillation, PV, gas stripping and liquid-liquid extraction. Among these processes, PV is recognized as an energy efficient alternative to distillation and other separating methods for liquid mixtures, especially where the traditional separation techniques are not efficient, such as the separation of azeotropic mixtures, isomeric components and close-boiling point systems [6-9]. Hydrophobic polymeric membranes, such as polydimethylsiloxane (PDMS) [10-13], polyether block amide (PEBA) [14,15], polyurethaneurea (PU) [16], poly(1-trimethylsilyl-1-propyne) (PTMSP) [17], and silicone rubber-coated silicalite membranes [18-20], as well as many mixed matrix membranes [21-26] have been tested for the recovery of *n*-butanol from aqueous solutions by pervaporation. Among the membrane materials stated above, the composite membranes concerning PDMS have been recognized as the most suitable candidate to separate organic compounds from water due to its low glass transition temperature and hydrophobicity. A typical preparation method of PDMS membrane is to cross-link α, ω-dihydroxypolydimethylsiloxane (H-PDMS) with a low molecular cross-linker, typically, tetraethoxysilicone (TEOS). This kind of PDMS membrane suffers from high bulk density, resulting in a large diffusion resistance to organic compounds. So it is desirable to prepare PDMS membranes with both high *n*-butanol permeability as well as satisfactory selectivity.

In recent years, hyperbranched polymers have been employed as novel membrane

separation materials. The highly branched dendritic structure entrusts them some excellent properties, such as lower package density, larger inter-molecular free volume, negligible crystallinity, *etc* [27, 28]. The tntroduction of hyperbranched structure into a membrane is rational to promote the diffusion of the permeants in membranes. For example, Wei and coworkers prepared hyperbranched poly (amine-ester) membranes cross-linked with 4, 4'-oxydiphthalic anhydride and glutaraldehyde, respectively. The membranes were used for isopropanol dehydration by PV [29]. Luo and coworkers synthesized an aliphatic type of hyperbranched polyester from 2, 2-dihydroxymethyl propanyl acid and 1, 1, 1-trihydroxymethyl propane and employed as the macromolecular cross-linking agents to enhance the pervaporation performance of ethyl cellulose membrane for the separation of benzene/cyclohexane mixtures. The membrane exhibited very large total flux and modest separation factor [30]. Unfortunately, owing to the relatively hydrophilic nature, the above mentioned membranes containing hyperbranched structure can neither be used to recover *n*-butanol from water directly nor blended with hydrophobic PDMS matrix. Therefore, membranes prepared with hyperbranched PDMS could be a good candidate for separation of *n*-butanol from water in PV process.

In the present paper, a hydrophobic cross-linker with hyperbranched structure, HPSiO, was synthesized and cross-linked with H-PDMS to prepare a new PDMS membrane for recovery of *n*-butanol from aqueous solutions. To optimize the membrane structure, three H-PDMS with different molecular weights were chosen to

prepare HPSiO-*c*-PDMS membranes and the effect of molecular weight of H-PDMS on the surface and inner physical structure was studied. Furthermore, their PV performances for separating *n*-butanol from water were intensively discussed according to the different membrane structures.

2. Experimental

2.1 Materials

Analytically pure sodium hydroxide, n-hexane and acetic acid were purchased from Shanghai Chemical Company, China and used as received. Vinyltriethoxysilane (VTES) of analytical grade was purchased from Sigma Chemical Co. Ltd., U.S.A. Dibutyltin dilaurate (DBTDL, catalyst) was purchased from Hangzhou Chemical Agent Co., Ltd., China. Polyvinylidene Fluoride (PVDF) ultrafiltration (UF) membrane used as support was kindly supplied by Wuxi Greenpure Membrane Science and Technology Co., Ltd. China. α, ω-Dihydroxypolydimethylsiloxane (H-PDMS) were purchased from Zhongxing Chenguang Chemical Research Institute Co. Ltd., China. Their weight average molecular weights (Mw) are 39000, 78000 and 310000, respectively, which were determined by gel permeation chromatography (GPC) (Waters 1515 isocratic pump, a column set consisting of three Waters Styragel® columns HR4, HR3, HR1 and a Waters 2414 differential refractive index detector), tetrahydrofuran was used as an eluent, and the calibration was performed with polystyrene standards.

2.2 Synthesis of HPSiO

HPSiO was synthesized by a three-step process. Firstly, sodium vinydiethoxysilanolate was prepared by the reaction of sodium hydroxide and VTES in toluene at 5 °C with stirring for 2 h followed by the distillation of toluene and the by-product, ethanol, of the reaction system under vacuum. Secondly, the obtained sodium vinydiethoxysilanolate was re-dissolved in toluene and a stoichiometric amount of acetic acid was added drop wisely for acidization at 0 °C. After filtering off the precipitates, sodium acetate, a yellow solution (vinyldiethoxysilanol) was obtained. Finally, the catalyst, DBTDL, with a weight ratio of 0.01 to vinyldiethoxysilanol, was then added into the above solution to react for 8 h at 60 °C. After that, toluene was distilled off to get a yellow liquid, which was HPSiO. The detailed synthetic processes of HPSiO were given in Scheme 1.

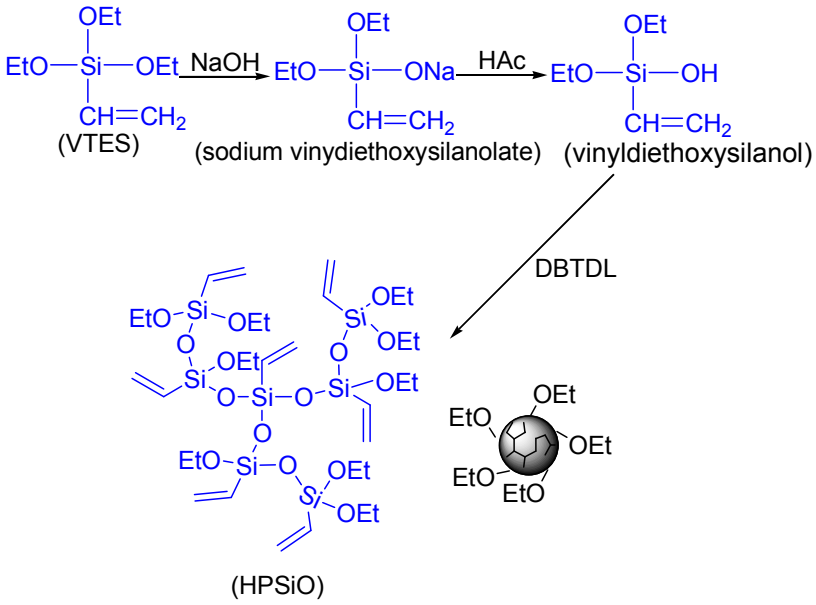

Scheme 1 Synthetic process of HPSiO

2.3 Preparation of HPSiO-c-PDMS Membranes

The cross-linked hyperbranched polysiloxane membranes, HPSiO-*c*-PDMS, were

prepared by solution casting method. [31] The casting solutions were prepared by the following method: H-PDMS with different molecular weights, HPSiO and catalyst DBTDL were mixed according to 7:3:0.01 weight ratio in n-hexane under vigorous stirring to form a viscous solution. After that, the solution was cast onto a polyvinylidene fluoride ultrafiltration membrane and kept at the ambient temperatures for 2 h for solvent evaporation followed by a 24 h thermal curing at 80 ^{o}C. For simplicity, the membranes cross-linked with H-PDMS with molecular weight of 39000, 78000 and 310000 were defined as HPSiO-*c*-PDMS-1, HPSiO-*c*-PDMS-2 and HPSiO-*c*-PDMS-3, respectively.

2.4 FT-IR

The chemical structures of vinyldiethoxysilanol and HPSiO were confirmed by Fourier Transform Infrared (FTIR) using a Brucker Vector22 type spectrometer. Samples for FTIR measurements were obtained by spreading a thin film of their casting solutions on a potassium bromide flake and evaporated the solvent n-hexane under vacuum at room temperature.

2.5 ^{29}Si NMR of HPSiO

^{29}Si NMR spectrum of HPSiO was obtained from Advance 500 (Bruker) at room temperature performing 2000 scans with a prescan delay of 12.5 s using 20 wt% in toluene (99.5%D GmBH) solutions containing 0.015 mol/L chromium (III) acetylacetonate (purum, Fluka) as a paramagnetic relaxing agent. Tetramethylsilane (puriss, Fluka) was used as an internal standard. The spectrum was corrected for the background signal from the probe by numerical subtraction of a baseline that was

recorded for the pure solvent.

2.6 Scanning Electron Microscope of HPSiO-c-PDMS Membranes

Scanning electron micrographs of HPSiO-*c*-PDMS membranes were performed on a Hitachi S4800 scan-ning electron microscope (SEM) instrument. All the samples were coated with a thin layer of gold to prevent charging.

2.7 Contact Angle Measurements of HPSiO-c-PDMS Membranes

Static contact angles of water on membranes were measured by sessile drop method [32, 33] using a contact angle meter (OCA 20, Dataphysics Instruments GmbH Germany) at 25 $^{\circ}$C and at about 65 % relative humidity. The volume of the water drops used was always 2 μL. All reported values were average of at least eight measurements taken at different locations of the film surface and had standard deviation of $\pm 1^{\circ}$.

2.8 Mechanical Properties of HPSiO-*c*-PDMS Membranes

The HPSiO-*c*-PDMS membranes were prepared by normal method in which the casting solution with concentration of 15g/50ml was poured onto a clean polytetrafluoroethylene (PTFE) plate and the evaporating temperature of the solvent was maintained at about 80 ^{o}C for 24 h. The dry membranes had about 300 μm in thickness. The stretching test of HPSiO-c-PDMS membranes was carried out at room temperature using an electronic universal testing machine (WCT-10). Specimens with an effective length of 40 mm (distance between the clamps) and a width of 5 mm were tested at a deformation rate of 20 mm min^{-1}. The average value of the tensile strength and elongation at break was determined on a series of 4-6 samples.

2.9 Degree of Swelling Measurement

The dried HPSiO-*c*-PDMS membranes without substrate were weighed and then immersed into aqueous solution of *n*-butanol with different concentration in a sealed vessel at 40 ^{o}C until equilibrium was reached. The swollen membranes were wiped out carefully with tissue paper to remove superficial liquid and weighted in a tightly closed bottle. The degree of swelling (*DS*) of the membrane was then determined from following equation:

$$DS = \frac{m_s - m_o}{m_o} \times 100\% \quad (1)$$

where m_0 and m_s are the weights of dry and swollen membranes, respectively.

2.10 Diffusion Coefficient of HPSiO-c-PDMS Membranes

The diffusion coefficient was recommended to describe the diffusion behavior of the HPSiO-*c*-PDMS membranes. The concentration-averaged diffusion coefficient of component i was calculated from Eq. (2) reported by Ma [34] and evolved from Fick's law of Eq. (3):

$$\overline{D_i} = \frac{J_i \delta}{C_i} \quad (2)$$

$$J_i = -D_i \frac{dC_i}{dx} \quad (3)$$

Where $\overline{D_i}$ represents concentration-averaged diffusion coefficient of component i (m^2/s), J_i is the flux of component i, C_i is the concentration (kg/m^3), δ is the membrane thickness, and x is the diffusion length (m).

2.11 Pervaporation Measurements

A typical pervaporation experimental process was shown in Fig. S1. More detailed

steps were shown in support information. The partial permeation flux (J_i) and the separation factor ($\beta_{sep,\ n\text{-butanol/water}}$) for all membranes were calculated according to the equations (4) and (5):

$$J_i = \frac{Q_i}{At} \tag{4}$$

$$b_{\text{sep,n-butanol/water}} = \frac{C_{\text{n-butanol}} / C_{\text{water}}}{x_{\text{n-butanol}} / x_{\text{water}}} \tag{5}$$

where Q_i is the weight of compound i in the permeate collected in time t, and A is the effective membrane area (35.24 cm^2). $x_{\text{n-butanol}}$ and x_{water} are the weight fractions of n-butanol and water in the feed side, and $C_{\text{n-butanol}}$ and C_{water} are the weight fractions in the permeate side, respectively. Based on the solution-diffusion model, the permeability (P^G_i) and selectivity ($\alpha_{n\text{-}butanol/water}$) can be calculated according to the equations (6) and (7):

$$P_i^G = J_i \frac{\delta}{P_{io} - P_{il}} \tag{6}$$

$$\alpha_{n-butanol/water} = \frac{P^G_{n-butanol}}{P^G_{water}} \tag{7}$$

where P_i^G is the membrane permeability for a compound i (Barrers, 1 Barrer 1×10^{-10} cm^3(STP) cm/cm^2 s cmHg). P_{io} and P_{il} are the vapor pressures of component i on the feed and permeate sides of the membrane [35, 36].

3. Results and discussion

3.1 Characterization of HPSiO

HPSiO was synthesized from an AB_2-type monomer vinyldiethoxysilanol and the ^{29}Si NMR spectrum of HPSiO was presented in Fig. 1. The ^{29}Si NMR spectrum of HPSiO showed four groups of peaks, which can be assigned to three types of

repeating units classified as dendritic, linear and terminal ones depending on the number of unreacted ethyoxy functional groups and residual un-reacted VTES, respectively. For simplicity, the four different groups were designated as Q_X, where X indicated the number of un-reacted ethoxy groups, ie, Q_0, no ethoxy groups (-108 ppm, 45%, dendritic units), Q_1, one ethoxy groups (-91 ppm, 26%, liner units), Q_2, two ethoxy groups (-74 ppm, 26%, terminal units), and Q_3, three ethoxy groups (-66 ppm, 3%, VTES). The areas of the individual peaks allow the estimation of the relative amounts of terminal, linear, and dendritic units in the different polymers. The degree of branching (*DB*), which was usually used as a factor to explain the structure of hyperbranched polymers was calculated according to the Eq. (8) [37]:

$$\text{Degree of branching}\,(DB) = \frac{D + T}{D + L + T} \tag{8}$$

where *D* is the number of dendritic units, *T* is the number of terminal units and *L* is the number of linear units. The calculated *DB* of HPSiO was 0.73, which means the mechanism was encouraging the branching process and a significant fraction of branched units were produced in the structure.

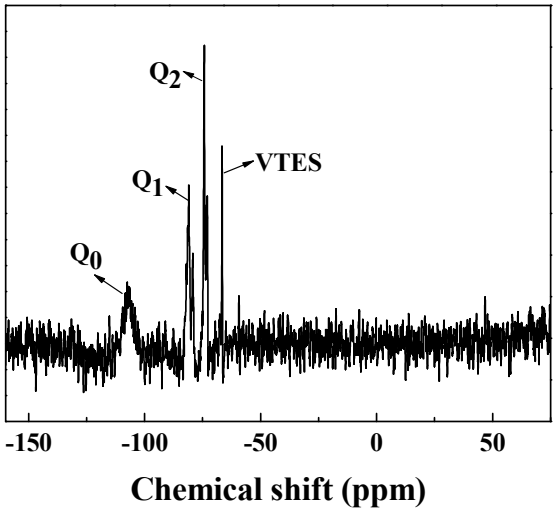

Fig.1 ^{29}Si NMR spectra of HPSiO

The FT-IR spectra of HPSiO and vinyldiethoxysilanol monomer were exhibited in Fig. 2. In the FT-IR spectrum of vinyldiethoxysilanol, a characteristic band appeared around 3400 cm^{-1} which is corresponding to the stretching vibrations of O-H and the band appeared at about 1100 cm^{-1} assigning to Si-O. There was no evidence of the characteristic peak relating to a free hydroxyl group near 3400 cm^{-1} in the spectrum of HPSiO, indicating nearly complete condensation of ethoxy groups in vinyldiethoxysilanol monomers.

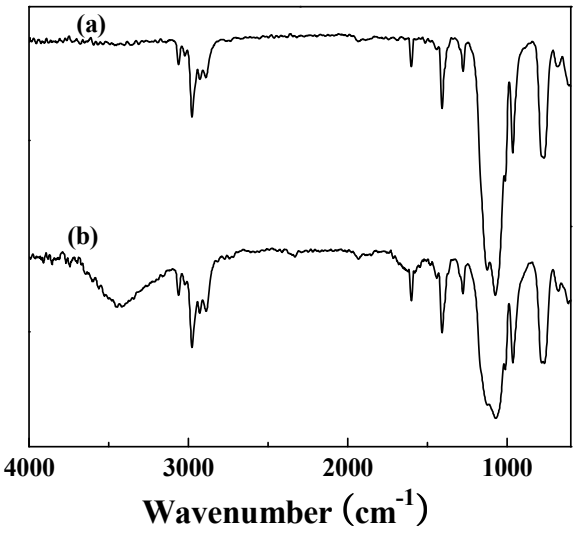

Fig.2 FT-IR spectra of (a) HPSiO and (b) vinyldiethoxysilanol

As listed in Table S1, the results from GPC analysis based on linear polystyrene standards gave a weight-averaged molecular weight (M_w) of HPSiO 3513 and the relative large polydispersity 2.48, which is owing to the fact that the molecular chain contains a lot of branched structure.

3.2 Mechanical Properties of HPSiO-c-PDMS Membranes

In order to study the effect of the molecular weight of H-PDMS on mechanical properties, the tensile strength and the elongation at break of HPSiO-*c*-PDMS-1, HPSiO-*c*-PDMS-2 and HPSiO-*c*-PDMS-3 were measured as shown in Table 1. From Table 1, the tensile strength demonstrated downtrend and the elongation at break of the HPSiO-*c*-PDMS membranes increased correspondingly with increasing the molecular weight of H-PDMS. Apparently, HPSiO-*c*-PDMS membrane with a higher H-PDMS molecular weight possesses more flexible molecular chains than that with a lower H-PDMS molecular weight. On the other hand, it can be inferred that in HPSiO-*c*-PDMS-1 membrane there are more crosslinkage than that in

HPSiO-*c*-PDMS-2 and HPSiO-*c*-PDMS-3 membranes. This is because that, for a fixed mass fraction in the HPSiO-*c*-PDMS membranes, there are fewer reacting points in H-PDMS with a larger molecular weight compared with the one with a lower molecular weight.

Table 1 Mechanical properties of HPSiO-*c*-PDMS membranes

Membranes	Tensile strength (MPa)	Elongation at break (%)
HPSiO-*c*-PDMS-1	2.95±0.2	709±5.2
HPSiO-*c*-PDMS-2	2.41±0.1	1451±6.3
HPSiO-*c*-PDMS-3	1.72±0.4	3561±10.9

3.3 Scanning Electron Microscope

The scanning electron micrographs of the surface and the cross-section of HPSiO-*c*-PDMS membranes were shown in Fig. S2 and Fig. 6. The thickness of all membranes is in a range of 20-30 μm. From Fig. S2 and Fig. 6, no appreciable pore could be observed, indicating that defect-free dense membrane was synthesized. It could be seen from Fig.6 (a-1) to (c-1) that HPSiOs were uniformly dispersed in the membrane matrix.

3.4 Swelling Behaviors of HPSiO-c-PDMS Membranes in n-Butanol Aqueous Solutions

The equilibrium degree of swelling (*DS*) of HPSiO-*c*-PDMS membranes in *n*-butanol aqueous solutions at 40 ^{o}C was illustrated in Fig. 3. It can be clearly seen that the equilibrium swelling degree of HPSiO-*c*-PDMS membranes increased with

the increase of *n*-butanol concentration in the feed solution. This is because the swelling of a polymer material in a solvent is proportional to its interaction or affinity with the solvent. [38, 39, 40] In addition, HPSiO-*c*-PDMS-3 exhibited the higher *DS* than the other two membranes. This is because HPSiO-*c*-PDMS-3 has more flexible molecular chains and lower crosslinking densities, which have lower resistance to the movement of *n*-butanol and water into the membrane.

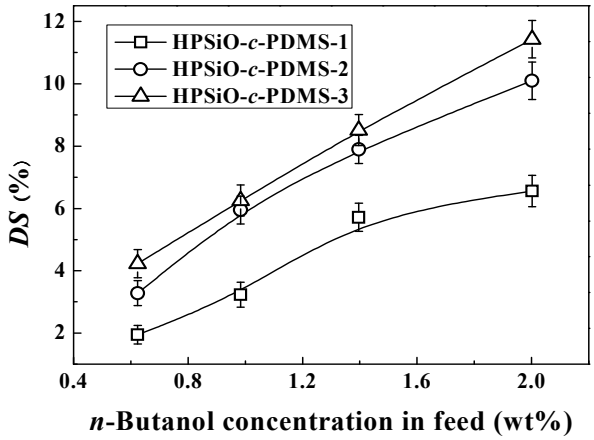

Fig.3 *DS* of HPSiO-*c*-PDMS membranes in *n*-butanol aqueous solutions at 40 ^{o}C

3.5 PV Performances of HPSiO-c-PDMS Membranes

3.5.1 Effect of H-PDMS molecular weight

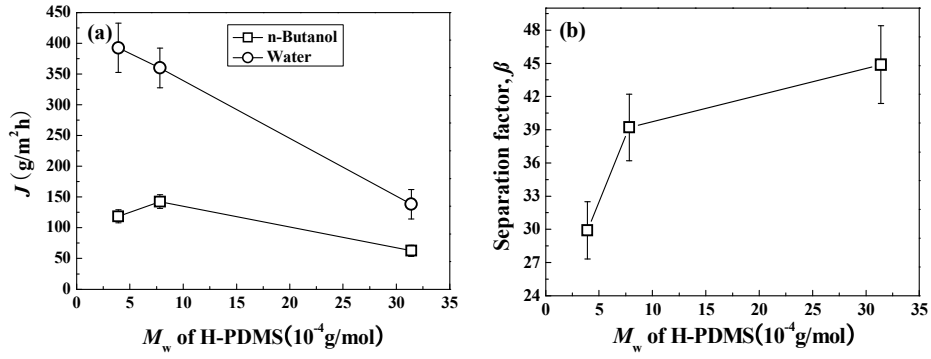

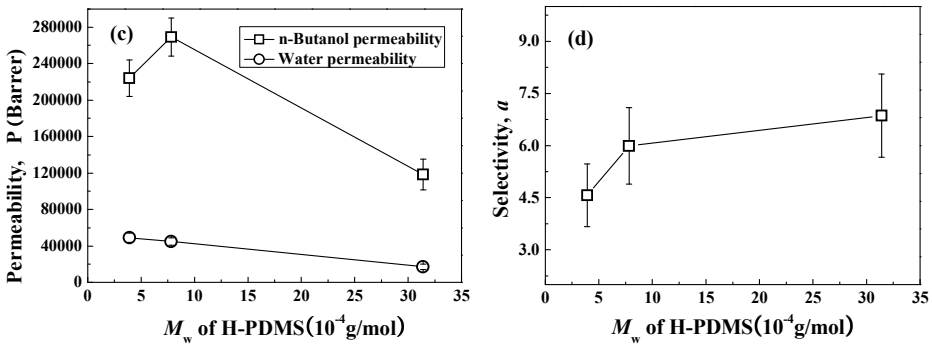

Fig.4 Effect of H-PDMS molecular weight on PV performance of HPSiO-*c*-PDMS membrane, (a) flux, (b) separation factor, (c) permeability and (d) selectivity

Fig. 4 shows the effect of H-PDMS molecular weight on the PV performances of HPSiO-*c*-PDMS membranes with a 1.0 wt% *n*-butanol aqueous solution at 40 ^{o}C. As shown in Fig. 4 (b), the separation factor increased from 29.91 to 44.88 with the H-PDMS molecular weight from 39000 to 310000, indicating that the HPSiO-*c*-PDMS membrane transported *n*-butanol over water, which will be precisely discussed later in this section. From Fig. 4 (a), with increasing H-PDMS molecular weight, the water flux continuously decreased while the *n*-butanol flux increased at the beginning and then decreased. A maximum value of *n*-butanol flux was found in HPSiO-*c*-PDMS-2 membrane, about 2.69×10^{5} Barrer. Water flux was larger than *n*-butanol flux in Fig. 4 (a), but *n*-butanol permeability was much larger than water permeability in Fig. 4 (c) after the fluxes (*n*-butanol and water) were normalized to permeabilities by taking into the account of the driving forces for permeation and membrane thickness. The trend of the selectivity shown in Fig. 4 (d) was consistent approximately to the variation of the separation factor of the HPSiO-*c*-PDMS membranes in Fig. 4 (b). In general, the PV performance for recovery of organic from

its aqueous solution is based on the solubility of permeates into a polymer membrane (sorption process) and the diffusivity of permeates in the polymer membrane (diffusion process). The solubility and diffusivity of permeates are significantly influenced by the chemical and physical structures of polymer membrane. First of all, in order to discuss the effect of H-PDMS molecular weight on the separation factor of HPSiO-*c*-PDMS membranes, the *n*-butanol concentration absorbed in the membranes with a 1.0 wt% *n*-butanol aqueous solution and the water contact angle were measured. As can be seen from Fig.S3, the water contact angles increased with increasing H-PDMS molecular weight in HPSiO-*c*-PDMS membranes, suggesting that hydrophobility of surface of HPSiO-*c*-PDMS membrane was escalated. The more hydrophobic membrane surface favored the absorption of *n*-butanol while repelling water from its surface. Moreover, the absorbed *n*-butanol concentration also increased with increasing H-PDMS molecular weight in the HPSiO-*c*-PDMS membranes. These two effects leaded to enhancement of the separation factor or selectivity with increasing H-PDMS molecular weight.

As for diffusion process, the diffusion coefficient of *n*-butanol and water with different H-PDMS molecular weight were measured, which is shown in Fig. 5. For the *n*-butanol, the diffusion coefficient increased at first and then descended, a maximum value of the diffusion coefficient was found in HPSiO-*c*-PDMS-2 membrane. But for water, the diffusion coefficient continuously decreased. From Fig. 5, for all HPSiO-*c*-PDMS membranes, the diffusion coefficients of *n*-butanol were about 10 times larger than those of water, indicating the HPSiO-*c*-PDMS membrane

was good for the transportation of *n*-butanol than for water. Both the declined diffusion coefficient of water and enhanced surface hydrophobicity in Fig. S3 caused the decline of water flux or permeability.

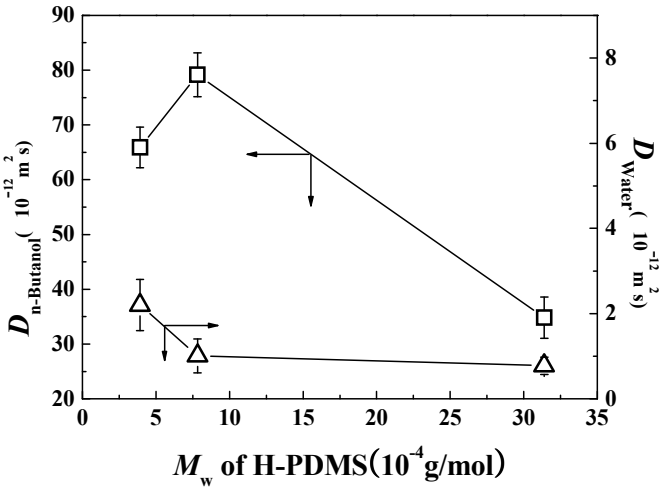

Fig.5 Effect of H-PDMS molecular weight on diffusion coefficient of n-butanol and water at 40 ^{o}C

According to the results from the Fig. 4 and Fig. 5, it is clearly known that the *n*-butanol and water permeabilities were mainly determined by diffusion of *n*-butanol and water in HPSiO-*c*-PDMS membranes. In order to explain this diffusion mechanism of *n*-butanol and water in HPSiO-*c*-PDMS membranes, hypothetical structures of HPSiO-*c*-PDMS membranes, based on the above experimental results from contact angles and diffusion coefficients, were shown in Fig. 6. In the model (a), due to low H-PDMS molecular weights, HPSiO is easy to react with Si-OH groups of H-PDMS, resulting in a high crosslinking density of a HPSiO-*c*-PDMS membrane. Despite the high crosslinking density could hinder the diffusion of *n*-butanol, but this negative effect is offset by existence of HPSiO in the HPSiO-*c*-PDMS membrane. As

can be seen in model (a), HPSiO was either existed at the surface or in the interior of the HPSiO-*c*-PDMS membrane. It could effectively increase the free volume of the HPSiO-*c*-PDMS membrane and decrease the package density of the HPSiO-*c*-PDMS membrane, thus facilitates the diffusion of *n*-butanol. Moreover, due to HPSiO was uniformly dispersed in the HPSiO-*c*-PDMS membrane, it would introduce extra channels to facilitate the diffusion of *n*-butanol through the membrane. So, the diffusion of *n*-butanol was still enhanced due to above two positive effects in spite of the negative effect caused by high crosslinking density. When H-PDMS molecular weights increased from 39000 to 78000, compared with HPSiO-*c*-PDMS-1 membrane in model (a), the structure of HPSiO-*c*-PDMS-2 (shown in model (b)) is almost unchanged, but the crosslinking density was declined. This would be more conducive to the diffusion of *n*-butanol. But when H-PDMS molecular weight was increased to 314043, the crosslinking density was sharply decreased, indicating that many HPSiOs are prone to "agglomeration" because of self-aggregation of HPSiOs. Meanwhile, PDMS chains are inclined to cover the surface of HPSiO, which can be seen in model (c). The former can't effectively improve the free volume of HPSiO-*c*-PDMS-3 membrane. Instead, the latter obviously increase the package density of HPSiO-*c*-PDMS-3 membrane. So, the diffusion of *n*-butanol is declined, compared with the HPSiO-*c*-PDMS-1 and HPSiO-*c*-PDMS-2. As for water, the contact angles were continually increased with increasing of H-PDMS molecular weights from Fig. S3, suggesting that the hydrophobicity of the membranes was increased, which was more prone to form water cluster, leading to the decline of the diffusion of water. [16,

32, 41] Through above analysis, it led us to consider that good diffusion performance is linked to appropriate crosslinking density and homogenous disperision of HPSiO in membrane.

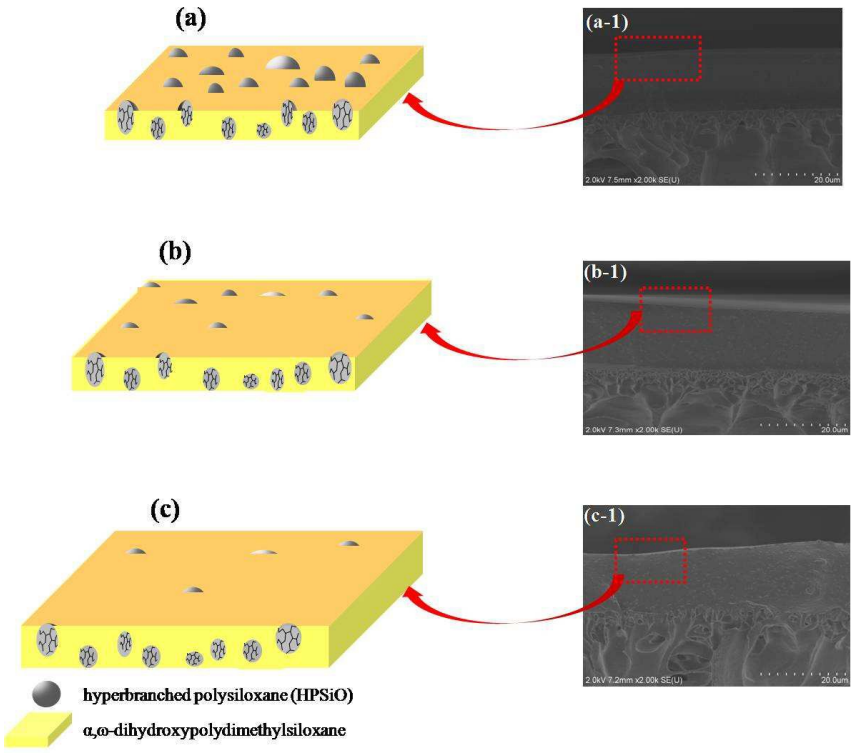

Fig.6 SEM images of the cross section and structure of the cross-linked HPSiO-*c*-PDMS membrane: (a) and (a-1) HPSiO-*c*-PDMS-1, (b) and (b-1) HPSiO-*c*-PDMS-2, (c) and (c-1) HPSiO-*c*-PDMS-3

3.5.2 Effect of Feed Temperature

Fig. 7 shows the variation of flux (a-1), permeability (a-2), separation factor (b-1) and selectivity (b-2) of HPSiO-*c*-PDMS-2 membrane with feed temperature (the feed concentration is 1.0 wt%). From Fig. 7 (a-2), it can be seen that both *n*-butanol and water permeability decreased with increasing the feed temperature while *n*-butanol permeability was changed more significantly than water permeability. As a result, the

selectivity of HPSiO-*c*-PDMS-2 membrane decreased from 8.75 at 30 ^{o}C to 3.27 at 60 ^{o}C in Fig. 7 (b-2). This phenomenon was also reported by Dong *et al*. [42] when PDMS/ZIF-8 membranes were used to separate *n*-butanol from *n*-butanol/water mixtures. They considered that it is attributed to negative effect caused by declining sorption outweighing positive effect caused by ascending diffusivity. In addition, higher activation energy of *n*-butanol ($E_{\text{n-butanol}}$=34.67 kJ/mol) than that of water (E_{water}=31.80 kJ/mol) in Fig. 8, indicating that the transport of *n*-butanol through HPSiO-*c*-PDMS-2 membrane was more sensitive to the temperature, ultimately also causes the decline of selectivity due to more decline in the permeability of *n*-butanol than water as the temperature increased. But, contrary to the variation of permeance versus temperature, *n*-butanol and water flux increased with feed temperature (Fig. 7 (a-1)). Guo *et al*. [43] also found this abnormal phenomenon when they studied difference between permeance and flux of polymeric membranes. They explained the phenomena being ascribed to the fact that the flux can not accurately reflect the temperature influence on transport performance, because it contains both the intrinsic membrane properties as well as external operational factors, such as activity coefficient and saturated vapor pressure. On the contrary, the permeance can reflect the true transport of the membrane due to removing the effects of operational factors. A similar conclusion was also reported by Richard *et al.* when they compared permeance with the flux of silicone rubber membranes. [35] They thought that the increase of flux with increasing temperature was completely due to the enhancement of vapor pressure driving force. The intrinsic permeance actually was decreased as

temperature increased.

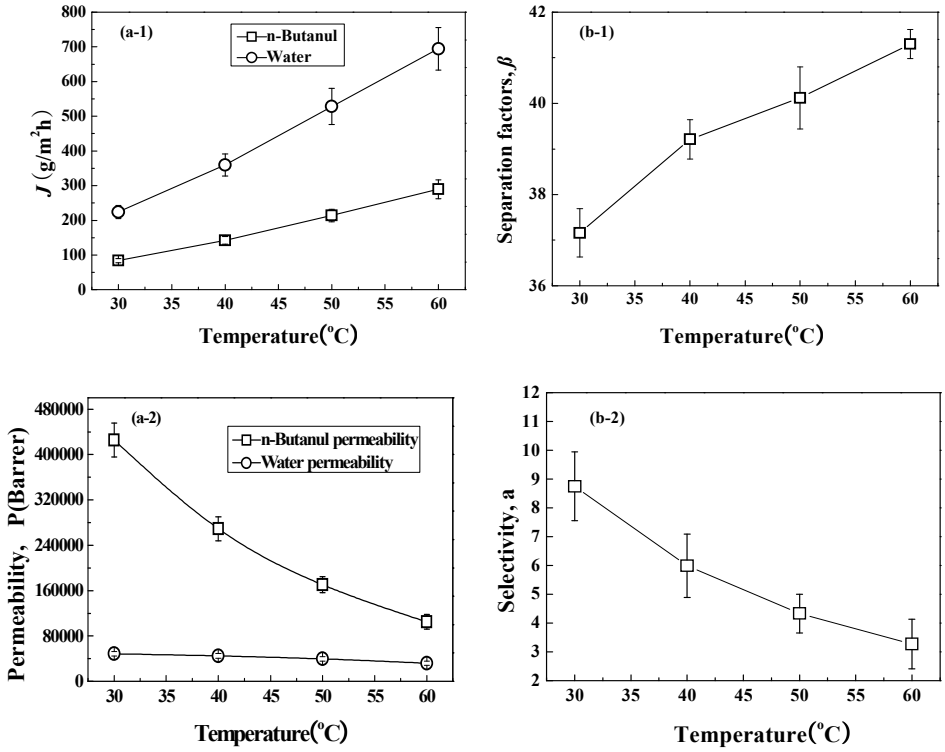

Fig.7 Effect of operating temperature on PV performance of HPSiO-*c*-PDMS-2 membrane, (a-1) flux, (b-1) separation factor, (a-2) permeability and (b-2) selectivity

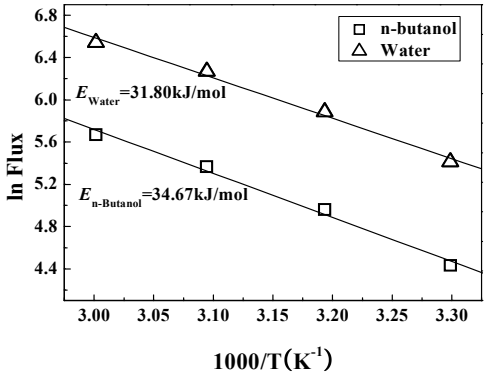

Fig.8 Arrhenius plot of HPSiO-*c*-PDMS-2 membrane for an aqueous solution of 1.0 wt% *n*-butanol.

3.5.3 Effect of Feed Concentration

Fig. 9 shows the variation of the permeability and selectivity of HPSiO-*c*-PDMS-2

membrane with the feed concentration from 0.5 to 2.0 wt% at 40 °C. From Fig. 9 (a-2) and (b-2), it can be seen that both permeability and selectivity are nearly unchanged with increasing feed concentration, while *n*-butanol flux were enhanced and the separation factor descended obviously in Fig. 9 (a-1) and (b-1). Wijmans [35] consider this difference between flux versus permeability and separation factor versus selectivity to be ascribed to the driving force across the membrane. The increase in flux with increasing feed concentration is mainly due to changes in permeates vapor pressure (driving force) with concentration. After the driving force effect was removed, the permeability would almost kept constant. Specific to this study, after *n*-butanol and water flux were normalized to permeability based on Eq (6), the *n*-butanol and water permeance were kept constant. In conclusion, compared with flux and the separation factor in Fig. 9 (a-1) and (b-1), the data in Fig. 9 (a-2) and (b-2) can reflect actual separation performance of a membrane due to eliminating the effect of operating conditions [44].

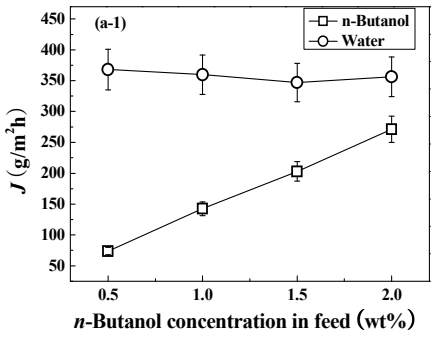

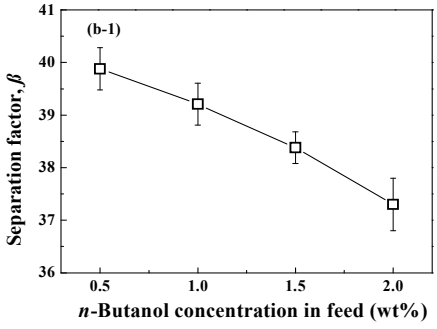

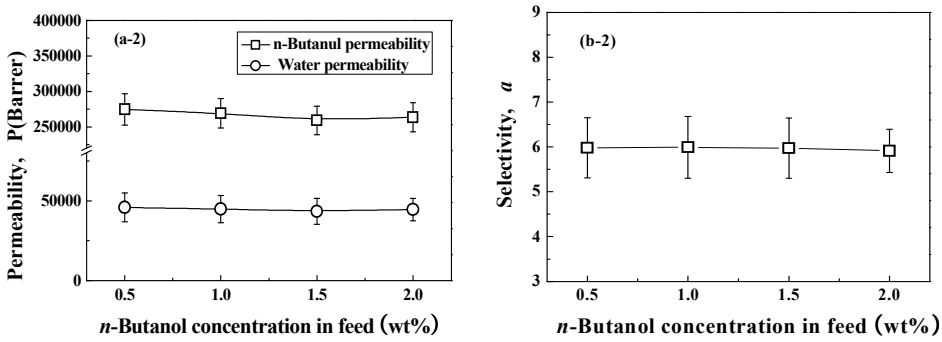

Fig.9 Effect of feed concentration on PV performance of HPSiO-*c*-PDMS-2 membrane, (a-1) flux, (b-1) separation factor, (a-2) permeability and (b-2) selectivity

3.6 Comparison of PV Performances of HPSiO-c-PDMS Membranes with Those in Literatures

Table 2 summarizes the PV performance of different membranes for *n*-butanol recovery from water in literatures. It is noticed that the cross-linked membranes based on hyperbranched polysiloxane in the present work have larger *n*-butanol flux than those of others' reported membranes except tri-layer PDMS [10] and PTMSP membrane [17]. PTMSP membrane has by far the highest *n*-butanol permeability among the known materials due to its large free volume, but the stability of PV performance should be improved. The selectivity of HPSiO-*c*-PDMS membrane is not outstanding enough compared with other membrane materials, but it may be improved by incorporating porous additives with *n*-butanol affinity, such as ZIF-8 [45]. The relative research work is conducting in our research group and will be reported in the future.

Table 2 Comparative study of PV performance of various membranes reported in the literature for recovery of *n*-butanol

Ref.	Membrane	Selectivity,α	Permeability of *n*-butanol ($\times 10^5$Barrer)	*T* (^{o}C)	C (wt%)	*m* (μm)
[10]	Tri-layer PDMS	5.20	1.49	40	1	65
[14]	PEBA	2.76	1.27	23	1	100
[16]	PTMSP	13.51	7.48	25	1	100
[18]	Silicalite-filled PDMS	1.84	1.09	40	1	306
[19]	PDMS	6.42	0.75	30	1	50
[19]	PERVAP-1070	10.37	1.14	40	1	29
[24]	Modified silicalite-filled PDMS	12.96	0.024	50	1	100
[42]	PDMS/ZIF-8	5.95	1.71	40	0.96	73
[46]	CMX-GF-010-D	5.96	0.88	40	1	10
[47]	PDMS–PAN	3.30	1.59	42	1	4.0
This work	HPSiO-*c*-PDMS-2	5.99	2.24	40	1	20

m: Membrane thickness, *T*: feed temperation, *C*: feed concentration, PTMSP: poly[1-(trimethylsilyl)-propyne], PERVAP-1070: silicalite-slicone composite

membrane provided by Sulzer Chemtech GmbH Membrane Systems of German, CMX-GF-010-D: polysiloxane, PEBA: Poly(ether-block-amide).

4. Conclusions

High *n*-butanol separation performance PV membranes, HPSiO-*c*-PDMS, were successfully prepared by cross-linking hydroxyl terminated PDMS of different molecular weights with a synthesized hyperbranched polysiloxane. All the HPSiO-*c*-PDMS membranes showed *n*-butanol permselective and relatively higher *n*-butanol permeability owing to the introduction of hyperbranched structure. The *n*-butanol/water selectivity increased as molecular weight of H-PDMS increased, while the n-butanol permeability of HPSiO-*c*-PDMS-2 membrane shows the highest value because hyperbranched polysiloxane is inclined to be covered by H-PDMS chains. The permeability and the selectivity of all the HPSiO-*c*-PDMS membranes decreased with the increase of feed temperature. As the feed concentration increased, the permeabilities and selectivities of HPSiO-*c*-PDMS membranes almost keep constant. The PV performance, in terms of the selectivity and the *n*-butanol permeability, HPSiO-*c*-PDMS-2 reached 8.75 and 4.3×10^5 Barrer, respectively, with a feed concentration of 1.0 wt% at 30 ^{o}C.

Acknowledgement

This research was financially supported by the National Nature Science Foundation of China (21106053), and the Industry-Academia-Research Joint Research Project of Jiangsu Province (BY2013015-28).

Nnmenclature

DS	swelling degree of membrane (%)
M_0	weight of dry membrane (g)
M_S	weight of swollen membrane at equilibrium (g)
D_i	diffusion efficient of component i (m^2/s)
J_i	flux of component i (kg/m^2s)
C_i	concentration of component i (kg/m^3)
δ	membrane thickness (m)
x	diffusion length (m)
Q_i	permeate weight of component i (g)
A	membrane area (m^2)
t	operating time (h)
x_i	weight fractions of component i in the feed side
C_i	weight fractions of component i in the permeate side
P_i^G	permeability of component i (Barrer)
P_{io}	vapor pressures of component i on the feed side of membrane
P_{il}	vapor pressures of component i on the permeate side of membrane
DB	degree of branching of HPSiO
D	the number of dendritic units of HPSiO,
T	the number of terminal units of HPSiO

L	the number of linear units of HPSiO
$E_{\text{n-butanol}}$	permeation activation energy of *n*-butanol
E_{water}	permeation activation energy of water

GREEK LETTERS

$\alpha_{n\text{-butanol/water}}$	selectivity
$\beta_{\text{sep, n-butanol/water}}$	separation factor

References:

1. S. D. Smet, S. Lingier and F. E. D. Prez, *Polym. Chem.*, 2014, **5**, 3163-3169.
2. M. Omidalia, A. Raisia and A. Aroujaliana, *Chem. Eng. Process.*, 2014, **77**, 22-29.
3. S. B. Bankar, S. A. Survase, H. Ojamo and T. Granström, *RSC Adv.*, 2013, **3**, 24734-24757.
4. T. Ezeji and N. H. P. *Biotechnol. Bioeng.*, 2007, **97**, 1460-1469.
5. N. Qureshi, S. Hughes, I. S. Maddox and M. A. Cotta, *Biosyst. Eng.*, 2005, **27**, 215-222.
6. J. Li, N. X. Wang, H. Yan, S. L. Ji and G. J. Zhang, *RSC Adv.*, 2014, **4**, 59750-59753.
7. Q. Zhao, J. W. Qian, Q. F. An, Q. Yang and Z. L. Gui, *ACS Appl. Mater. Interfaces.*, 2009, **1**, 90-96.
8. J. W. Chen, H. Huang, L. Zhang and H. M. Zhang, *RSC Adv.*, 2014, **4**, 24126-24130.

9. M. G. Buonomenna, *RSC Adv.*, 2013, **3**, 5694-5740.

10. S. Y. Li, R. Srivastava and R. S. Pranas, *J. Membr. Sci.*, 2010, **363**, 287-294.

11. T. Aouak, S. Moulay and A. H. Ziane, *J. Membr. Sci.*, 20001, **73**, 149-157.

12. H. Benguergoura, T. Aouak and S. Moulay, *J. Membr. Sci.*, 2004, **229**, 107-116.

13. R. Anna, N. Johanna, L. K. Riitta and K. Wojciech, *J. Membr. Sci.*, 2014, **453**, 108-118.

14. E. A. Fouad, X. S. Feng, *J. Membr. Sci.*, 2008, **323**, 428-435.

19. T. Mohammadi, T. Kikhavandi and M. Moghbeli, *J. Appl. Polym. Sci.*, 2008, **107**, 1917-1923.

20. C. C. Tong, Y. X. Bai, J. P. Wu, L. Zhang, L. R. Yang and J. W. Qian, *Sep. Sci. Technol.*, 2010, **45**, 751-761.

21. H. Essawy, M. Tawfik, S. E. Sabbagh, A. E. Gendi, E. E. Zanati and H. Abdallah, *Polym.Eng. Sci.*, 2014, **54**, 1560-1570.

22. T. Ikegami, H. Negishi and K. Sakaki, *J. Chem. Technol. Biotechnol.*, 2011, **6**, 845-851.

23. N. Qureshi, M. M. Meagher and R. W. Hutkins, *J. Membr. Sci.*, 1999, **158**, 115-125.

24. J. C. Huang and M. M. Meagher, *J. Membr. Sci.*, 2001, **192**, 231-242.

25. X. L. Liu, Y. S. Li, G. Q. Zhu, J. Liu and W. S. Yang, *J. Membr. Sci.*, 2011, **369**, 228-232.

26. A. Dobrak, A. Figoli, S. Chovau, F. Galiano, S. Simone, I. F. J. Vankelecom, E. Drioli and B. V. D. Bruggen, *J. Colloid Interf. Sci.*, 2010, **346**, 254-264.

27. L. M. Vane, V. V. Namboodiri and R. G. Meier, *J. Membr. Sci.*, 2010, **364**, 102-110.

28. I. F. J. Vankelecom, D. Depre, S. D. Beukelaer and J. B. Uytterhoeven, *J. Phys. Chem.*, 1995, **99**, 13193-13197.

29. H. L. Zhou, Y. Su, X. G. Chen, S. L. Yi and Y. H. Wan, *J. Membr. Sci.*, 2010, **75**, 286-294.

30. X. L. Liu, Y. S. Li, Y. Liu, G. Q. Zhu, J. Liu and W. S. Yang, *J. Membr. Sci.*, 2011, **369**, 228-232.

31. Y. Segawa, T. Higashihara and M. Ueda, *Polym. Chem.*, 2013, **4**, 1746-1759.

32. Z. M. Dong and Z. B. Ye, *Polym. Chem.*, 2012, **3**, 286-301.

33. X. Z. Wei, X. F. Liu, B. K. Zhu and Y. Y. Xu, *Desalination*, 2009, **247**, 647-656.

34. Y. J. Luo, W. Xin, G. P. Li, Y. Yang, J. R. Liu, Y. Lv and Y. B. Jiu, *J. Membr. Sci.*, 2007, **303**, 183-193.

35. Q. Zhao, Q. F. An, Z. W. Sun, J. W. Qian, K. R. Lee, C. J. Gao and J. Y. Lai, *J. Phys. Chem. B.*, 2010, **114**, 8100-8106.

36. J. Gu, Y. X. Bai, L. Zhang, L. R. Deng, C. F. Zhang, Y. P. Sun and H. L. Chen, *Int. J. Polym. Sci.*, 2013, **2013**, 1-7.

37. J. Gu, X. R. Zhang, Y. X. Bai, L. Yang, C. F. Zhang and Y. P. Sun, *Int. J. Polym. Sci.*, 2013, **2013**, 1-10.

38. X. C. Ma, C. L. Hu, R. L. Guo, X. Fang, H. Wu and Z. Y. Jiang, *Sep. Purif. Technol.*, 2008, **59**, 34-42.

39. R. W. Baker and J. G. Wijmans, Y. Huang, *J. Membr. Sci.* 2010, **348**, 346-352.

40. H. J. Kim, N. A. Brunelli, A. J. Brown, K. S. Jang, W. G. Kim, F. Rashidi, J. R. Johnson, W. J. Koros, C. W. Jones and S. Nair, *ACS Appl. Mater. Interfaces.*, 2014, **6**, 17877-17886.

41. M. Jikei and M. Kakimoto, *Prog. Poly. Sci.* 2001, **26**, 1233-1285.

42. Q. Zhao, J. W. C. Dunlop, X. L. Qiu, F. H. Huang, Z. B. Zhang, J. Heyda, J. Dzubiella, M. Antonietti and J. Y. Yuan, *Nat. Commun.*, 2014, **5**,4293.

43. Q. F. An, J. W. Qian, Q. Zhao and C. J. Gao, *J. Membr. Sci.*, 2008, **313**, 60-67.

44. T. Liu, Q. F. An, Q. Zhao, K. R. Lee, B. K. Zhu, J. W. Qian and C. J. Gao, *J. Membr. Sci.*, 2013, **429**, 181-189.

45. R. Y. M. Huang, P. H. Shao, X. Feng and W. A. Anderson, *Ind. Eng. Chem. Res.*, 2002, **41**, 2957-2965.

46. Y. X. Bai, L. L. Dong, C. F. Zhang and J. Gu, *Sep. Sci. Technol.*, 2013, **48**, 2531-2539.

47. W. F. Guo, T. S. Chung and M. Takeshi, *J. Membr. Sci.*, 2004, **245**, 199-210.

48. J. G. Wijmans, *J. Membr. Sci.*, 2003, **220**, 1-3.

49. X. L. Liu, Y. S. Li, G. Q. Zhu, Y. J. Ban, L. Y. Xu and W. S. Yang, *Angew. Chem. Int. Ed.*, 2011, **50**, 10636-10639.

50. V. García, E. Pongrácz, E. Muurinen and R. L. Keiski, *Desalination*, 2009, **241**, 201-211.

51. N. Johanna, K. Wojciech and L. K. Riitta, *J. Membr. Sci.*, 2013, **434**, 55-64.

Caption of Figures:

Fig.1 ^{29}Si NMR spectra of HPSiO

Fig.2 FT-IR spectra of (a) HPSiO and (b) vinyldiethoxysilanol

Fig.3 DS of HPSiO-*c*-PDMS membranes in *n*-butanol aqueous solutions at 35 ^{o}C

Fig.4 Effect of H-PDMS molecular weight on PV performance of HPSiO-*c*-PDMS membrane, (a) flux, (b) separation factor, (c) permeability and (d) selectivity

Fig.5 Effect of H-PDMS molecular weight on diffusion coefficient of n-butanol and water at 40 ^{o}C

Fig.6 SEM images of the cross section and structure of the cross-linked HPSiO-*c*-PDMS membrane: (a) and (a-1) HPSiO-*c*-PDMS-1, (b) and (b-1) HPSiO-*c*-PDMS-2, (c) and (c-1) HPSiO-*c*-PDMS-3

Fig.7 Effect of operating temperature on PV performance of HPSiO-*c*-PDMS-2 membrane, (a-1) flux, (b-1) separation factor, (a-2) permeability and (b-2) selectivity

Fig.8 Arrhenius plot of HPSiO-*c*-PDMS-2 membrane for an aqueous solution of 1.0 wt% *n*-butanol.

Fig.9 Effect of feed concentration on PV performance of HPSiO-*c*-PDMS-2 membrane, (a-1) flux, (b-1) separation factor, (a-2) permeability and (b-2) selectivity